International Core Journal of Engineering Volume 10 Issue 5, 2024
ISSN: 2414-1895 DOI: 10.6919/ICJE.202405_10(5).0037

Reliability Assessment of Integrated Electricity and Heat Systems Considering Multi-Time Scale

Taihao Liu*

School of Electrical Engineering and Automation, Henan Polytechnic University, Jiaozuo 454003, China

*2010967607@qq.com

Abstract

In the reliability assessment, the reliability index of the unified time scale and the one-step state transition model of the Markov chain are usually used to calculate the state probability of the element, and the influence of multi-step state transfer and multi-time scale on the reliability assessment of the integrated electricity and heat systems is considered. Firstly, the multi-time probability model of multi-step state transition is derived by using the Markov chain Monte Carlo method, and a multi-time scale scheduling framework is established due to the different scheduling times of the subsystem, and the seven-interval approximation model of Gaussian distribution is used to predict the fluctuation of the load, and the seven-state uncertainty model of the load is established. Then, the system reliability evaluation index is established and a reliability evaluation method considering multiple time scales is proposed. Finally, the simulation results show that the proposed method can perform global calculations on the system, reduce the number of heat source output adjustments, avoid unnecessary calculations, and analyze the influence of load correlation and state transfer times on system reliability.

Keywords

Reliability Assessment; Integrated Electricity and Heat Systems (IEHS); Multi-Step State Transition; Multi-Time Scale; Reliability Assessment.

1. Introduction

The integration of a large number of new energy into the grid has played a certain role in alleviating the energy crisis and improving the environment, but it has brought threats to the reliability of the power system [1]. The integrated electricity and heat systems (IEHS), which couples the power and heat systems through combined heat and power (CHP) units and electric heat pump (EHP) units, are an effective way to solve the problem of new energy consumption and improve energy utilization [2]. However, since the randomness of energy measurement and load side poses a risk to the safe and reliable operation of IEHS, it is necessary to study the reliability evaluation of IEHS while taking into account the source-load uncertainty [3].

At present, some research has been carried out on the reliability assessment of comprehensive energy systems containing renewable energy at home and abroad. In reference [4], based on the Markov chain Monte Carlo (MCMC) method, the reliability of the integrated energy system was quantitatively evaluated by the value of the importance index. In reference [5], considering the uncertainty of the load, a scenario-based cogeneration scheduling model was proposed to calculate the node reliability index, and the hydrothermal decomposition technology based on the general generation function was used to effectively improve the calculation rate of IEHS reliability

ISSN: 2414-1895 DOI: 10.6919/ICJE.202405_10(5).0037

assessment. In reference [6], a comprehensive energy system reliability assessment method based on the sequential Monte Carlo simulation method is proposed, and the influence of PV output correlation, load reduction strategies considering users' thermal comfort, and demand response and coupling operation on the reliability assessment results are analyzed. In reference [7], a method for evaluating the operational reliability of the grid-connected system of Markov chain wind power is proposed, which takes into account the uncertainty factors of source-grid-load, and the influence of random variable fluctuations on the reliability of the system is quantitatively analyzed and compared. In reference [8], a comprehensive energy system reliability index and evaluation method that takes into account the thermal inertia of the load and the thermal comfort of the user are proposed, and the impact of photovoltaic correlation and load reduction strategy on the system reliability is analyzed.

On the basis of the above research, this paper considers the influence of multi-step state transition and multi-time scale on the reliability assessment of electric and thermal integrated energy system, establishes a multi-step state transition probability model, and proposes an IEHS optimal load reduction model and reliability evaluation method considering multiple time scales. The effectiveness of the proposed model and proposed method is verified by case analysis, and the influence of load correlation and state transition steps on the reliability of IEHS is analyzed. The simulation results can provide a certain reference for the study of the reliability of integrated energy systems.

2. MCMC Method, Multi-Time Scale Scheduling, and Load Uncertainty Model

2.1 The MCMC Method Considering Multi-Step State Transition

In order to reduce the calculation in reliability evaluation, the one-step state transition is usually used and the multi-step state transition is ignored, this section explores the state probability of the multi-step transition of the two-state Markov model to predict the state probability of the component, and the state transition process is shown in Figure 1, p_{00}, p_{01}, p_{10}, p_{11} represent the probability of the component being transferred between state 0 and state 1 and must meet $p_{00}+p_{01}=1$, $p_{10}+p_{11}=1$.

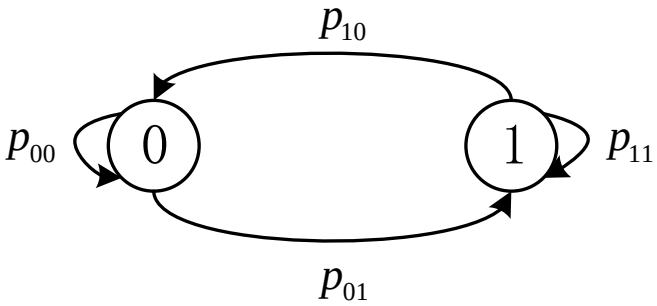

Figure 1. Two-state Markov model

Suppose, $p_{01}=\lambda$, $p_{10}=\mu$, then the one-step state transition matrix p.

$$\boldsymbol{p}=\begin{bmatrix} p_{00} & p_{01} \\ p_{10} & p_{11} \end{bmatrix}=\begin{bmatrix} 1-\lambda & \lambda \\ \mu & 1-\mu \end{bmatrix} \tag{1}$$

The n-th step state transition matrix P(n) is shown in equation (2).

ISSN: 2414-1895 DOI: 10.6919/ICJE.202405_10(5).0037

$$\boldsymbol{P}(n)=\begin{bmatrix} \dfrac{\mu+\lambda(1-\lambda-\mu)^n}{\lambda+\mu} & \dfrac{\lambda-\lambda(1-\lambda-\mu)^n}{\lambda+\mu} \\ \dfrac{\mu-\mu(1-\lambda-\mu)^n}{\lambda+\mu} & \dfrac{\lambda+\mu(1-\lambda-\mu)^n}{\lambda+\mu} \end{bmatrix} \tag{2}$$

To obtain the probability of each state at time t, the following system of differential equations is solved:

$$\begin{cases} \dfrac{\mathrm{d}p_0(t)}{\mathrm{d}t}=-\lambda_n p_0(t)+\mu_n p_1(t) \\ \dfrac{\mathrm{d}p_1(t)}{\mathrm{d}t}=\lambda_n p_0(t)-\mu_n p_1(t) \end{cases} \tag{3}$$

Where: λ_n is the failure probability of the n-th step state 0 to state 1; μ_n is the repair probability of the n-th step state 1 to state 0.

The initial state is $p_0(0)=1$, $p_1(0)=0$. Equation (4) is derived from the Laplace transform.

$$\begin{cases} p_0(t)=\dfrac{\mu_n}{\lambda_n+\mu_n}+\dfrac{\lambda_n}{\lambda_n+\mu_n}\mathrm{e}^{-(\lambda_n+\mu_n)t} \\ p_1(t)=\dfrac{\lambda_n}{\lambda_n+\mu_n}-\dfrac{\lambda_n}{\lambda_n+\mu_n}\mathrm{e}^{-(\lambda_n+\mu_n)t} \end{cases} \tag{4}$$

Where: $p_0(t)$ and $p_1(t)$ are the probabilities of the components in the running state and the fault state when the system is running from the start time t=0, respectively. Assuming that a component failure is unrepairable and an n-step transfer is carried out in a running cycle, that is, when the repair probability is 0, the component outage probability is:

$$p(t)=1-\mathrm{e}^{-\lambda_n t}=1-\mathrm{e}^{-[1-(1-\lambda)^n]t} \tag{5}$$

For each component, the Monte Carlo method is used to produce a uniformly distributed random number R_t between [0,1], if between [0, $p(t)$], it means that the component is faulty, otherwise the component can be considered to be in normal working condition, and it can be operated in state s_t for a long time.

$$s_t=\begin{cases} 1\ \text{(Fault state)} & 0\le R_t\le p(t) \\ 0\ \text{(Run state)} & R_t>p(t) \end{cases} \tag{6}$$

2.2 Multi-Time Scale Scheduling

Because the execution time of the optimal scheduling of the thermal system is relatively long, if the unified scheduling time is used in the scheduling, the system cannot operate efficiently. Here set the scheduling time of the thermal system and the power system to t_h and t_e, in order to facilitate the

ISSN: 2414-1895 DOI: 10.6919/ICJE.202405_10(5).0037

study, let $t_h / t_e = N \in R$, and repeat the scheduling process and implement it in the subsequent time window once the current scheduling period has concluded. When the total time of the optimization scheduling is the same as the execution time of the thermal system scheduling, the optimization scheduling is stopped and the scheduling end instruction is sent, as shown in Figure 2.

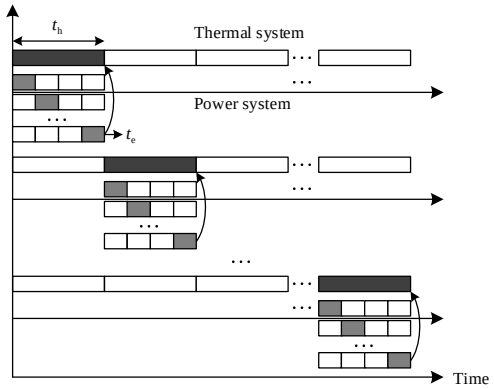

Figure 2. IEHS multi-timescale scheduling framework

The specific embodiment can be divided into the following two situations:

Scenario 1: When $T_e < T_h$, the thermal system's response to the control command remains ongoing, while the power system independently carries out rolling optimization scheduling. At this juncture, the level of state coupling with the thermal system remains stable relative to the power system. As a result, the boundary state of the power system can be directly ascertained based on the state of the thermal system and the pertinent boundary coupling conditions.

Scenario 2: When $T_e \geq T_h$, the scheduling times of the power system and the thermal system overlap, necessitating the updating of the boundary coupling parameters. Subsequently, each subsystem proceeds to the subsequent optimal scheduling time period.

2.3 Load Uncertainty Model

Generally speaking, the Gaussian distribution can well reflect the fluctuation of electricity and heat loads, the division and probability of each interval are shown in Figure 3, and the upper and lower limits of each interval are shown in equation (7).

$$\begin{cases} u_c = d_F + (c-4)\sigma_d + (1/2)\sigma_d \\ l_c = d_F + (c-4)\sigma_d - (1/2)\sigma_d \end{cases} \quad c = 1, 2, \cdots, 7 \tag{7}$$

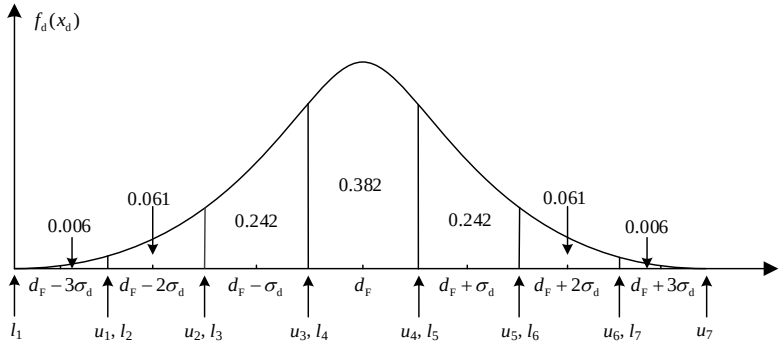

Figure 3. Seven-interval approximation of Gaussian distribution

ISSN: 2414-1895 DOI: 10.6919/ICJE.202405_10(5).0037

On this basis, this section also considers that the change of the actual load at adjacent times should be within a reasonable range, that is, the electric and heat loads should also meet equation (8).

$$\begin{aligned} -\sigma_{\mathrm{e}} \le P_{t+1}^{\mathrm{LD}} - P_{t}^{\mathrm{LD}} \le \sigma_{\mathrm{e}} \\ -\sigma_{\mathrm{h}} \le Q_{\tau+1}^{\mathrm{LD}} - Q_{\tau}^{\mathrm{LD}} \le \sigma_{\mathrm{h}} \end{aligned} \tag{8}$$

Where: σ_{e} and σ_{h} are the standard deviations of the electrical and thermal loads, respectively.

3. IEHS Optimal Load Reduction Model Considering Multi-Time Scales

If the load demand cannot be met by adjusting the output of the unit after a faulty component occurs in the IEHS, load reduction measures should be taken in time. Therefore, an optimal load reduction model is established to minimize the sum of the weights of electricity and heat load reduction in the scheduling of different time scales of the subsystem. The objective function is:

$$\min\left(\sum_{t=1}^{\mathrm{T_e}} \sum_{i=1}^{\mathrm{N_e}} \omega_{\mathrm{e},i} C_{i,t}^{\mathrm{E}} + \sum_{\tau=1}^{\mathrm{T_h}} \sum_{n=1}^{\mathrm{N_h}} \omega_{\mathrm{h},n} C_{n,\tau}^{\mathrm{H}} \right) \tag{9}$$

Where: $C_{i,t}^{\mathrm{E}}$ and $C_{n,\tau}^{\mathrm{H}}$ are the load shedding of the power system node i and the thermal system node n, respectively; $\mathrm{N_e}$ and $\mathrm{N_h}$ are the number of nodes of the power system and the thermal system, respectively; ω_{e} and ω_{h} are the weights of electrical and thermal energy in the total energy in the system, respectively.

The constraints of IEHS mainly include thermal system constraints, power system constraints, and coupling element constraints.

3.1 Power System Constraints

Power systems typically use an optimal power flow model based on DC power flow.

$$P_{i,t}^{\mathrm{W}} + P_{i,t}^{\mathrm{pv}} + P_{i,t}^{\mathrm{CHP}} + P_{i,t}^{\mathrm{G}} - P_{i,t}^{\mathrm{EHP}} = P_{i,t}^{\mathrm{LD}} - C_{i,t}^{\mathrm{E}} \tag{10}$$

$$P_{ij} = (\theta_i - \theta_j) / X_{ij} \tag{11}$$

$$0 \le C_{i,t}^{\mathrm{E}} \le P_{i,t}^{\mathrm{LD}} \tag{12}$$

$$-P_{\mathrm{L}}^{\max} \le P_{t}^{\mathrm{L}} \le P_{\mathrm{L}}^{\max} \tag{13}$$

$$0 \le P_{i,t}^{\mathrm{G}} \le P_{i}^{\mathrm{G,max}} \tag{14}$$

Where: $P_{i,t}^{\mathrm{W}}$, $P_{i,t}^{\mathrm{pv}}$, $P_{i,t}^{\mathrm{CHP}}$, $P_{i,t}^{\mathrm{G}}$, $P_{i,t}^{\mathrm{EHP}}$, $P_{i,t}^{\mathrm{L}}$ are respectively the power generation power of the wind turbine at node i, the power generation power of photovoltaic power generation, the power generation power of CHP unit, the power generation power of conventional unit, the power consumption power of EHP unit, and the transmission power of transmission line; θ_i is the voltage phase angle of node

ISSN: 2414-1895 DOI: 10.6919/ICJE.202405_10(5).0037

i; X_{ij} is the reactance from node i to node j of the transmission line; $P_{\mathrm{L}}^{\max}$ is the rated capacity of the transmission line.

3.2 Thermal System Constraints

Thermal system constraints include hydraulic and thermal model constraints:

$$\sum_{q\in\psi_{\mathrm{T},n}} m_{q,\tau} + m_{n,\tau}^{\mathrm{G}} = \sum_{q\in\psi_{\mathrm{F},n}} m_{q,\tau} + m_{n,\tau}^{\mathrm{L}} \tag{15}$$

$$\Delta p_{q,\tau} = K_q m_{q,\tau} \left| m_{q,\tau} \right| \tag{16}$$

$$\sum_{q\in\psi_{\mathrm{loop}}} \boldsymbol{B}\Delta p_{q,\tau} = 0 \tag{17}$$

Where: $\psi_{\mathrm{T},n}$, $\psi_{\mathrm{F},n}$, ψ_{loop} are respectively the collection of pipes flowing from the inflow node n and the collection of pipes flowing out from node n, forming the pipe collection of the loop; m_q is the supply/return water flow rate of pipeline q; $m_{n,t}^{\mathrm{G}}$ and $m_{n,t}^{\mathrm{L}}$ is the heat source and load water flow rate at node n; $\Delta p_{q,t}$ is the pressure loss of the supply/return loop of pipeline q; K_q is the drag coefficient of pipe q; B is the loop correlation matrix.

The thermal model constraints are as follows:

$$Q_{n,\tau} = \mathrm{C_p}\, m_{n,\tau}^{\mathrm{G}} (TS_{n,\tau}^{\mathrm{G}} - TR_{n,t}^{\mathrm{G}}) - C_{n,\tau}^{\mathrm{H}} \tag{18}$$

$$Q_{n,\tau}^{\mathrm{CHP}} + Q_{n,\tau}^{\mathrm{EHP}} = Q_{n,\tau}^{\mathrm{LD}} - C_{n,\tau}^{\mathrm{H}} \tag{19}$$

$$TS_{q,\tau}^{\mathrm{OUT}} = (TS_{q,\tau}^{\mathrm{IN}} - \mathrm{T}_{q,\tau}^{\mathrm{a}})\, \mathrm{e}^{-\lambda_q L_q/(\mathrm{C_p}\, \boldsymbol{m}_{q,\tau}^{\mathrm{SU}})} + \mathrm{T}_{q,\tau}^{\mathrm{a}} \tag{20}$$

$$TR_{q,\tau}^{\mathrm{OUT}} = (TR_{q,\tau}^{\mathrm{IN}} - \mathrm{T}_{q,\tau}^{\mathrm{a}})\, \mathrm{e}^{-\lambda_q L_q/(\mathrm{C_p}\, \boldsymbol{m}_{q,\tau}^{RE})} + \mathrm{T}_{q,\tau}^{\mathrm{a}} \tag{21}$$

$$\sum_{q\in\psi_{\mathrm{F},n}} m_{q,\tau}^{\mathrm{SU}} TS_{q,\tau}^{\mathrm{OUT}} + m_{n,\tau}^{\mathrm{G}} TS_{n,\tau}^{\mathrm{G}} = TS_{n,\tau} \Big(\sum_{q\in\psi_{\mathrm{T},n}} m_{q,\tau}^{\mathrm{SU}} + m_{n,\tau}^{\mathrm{G}} \Big) \tag{22}$$

$$\sum_{q\in\psi_{\mathrm{F},n}} m_{q,\tau}^{\mathrm{RE}} TR_{q,\tau}^{\mathrm{IN}} + m_{n,\tau}^{\mathrm{L}} TR_{n,\tau}^{\mathrm{L}} = TR_{n,\tau} \Big(\sum_{q\in\psi_{\mathrm{T},n}} m_{q,\tau}^{\mathrm{RE}} + m_{n,\tau}^{\mathrm{L}} \Big) \tag{23}$$

Where: $Q_{n,\tau}$ is the emitted power of the heat source at node n; $Q_{n,\tau}^{\mathrm{EHP}}$ is the heat power generated by the EHP unit at node n; $\mathrm{C_p}$ is the specific heat capacity of water; $TS_{n,\tau}^{\mathrm{G}}$, $TR_{n,\tau}^{\mathrm{G}}$, $TS_{n,\tau}^{\mathrm{L}}$, $TR_{n,\tau}^{\mathrm{L}}$ are the water supply temperature of the heat source of node n, the return temperature of the heat source, the load water supply temperature, and the load return water temperature, respectively; λ_q is the thermal

ISSN: 2414-1895 DOI: 10.6919/ICJE.202405_10(5).0037

conductivity coefficient of pipe q; L_q represents the length of the pipe q; $TS_{q,\tau}^{\mathrm{IN}}$, $TS_{q,\tau}^{\mathrm{OUT}}$, $TR_{q,\tau}^{\mathrm{IN}}$, $TR_{q,\tau}^{\mathrm{OUT}}$ are the inlet temperature and outlet temperature of the supply pipeline q, and the inlet temperature and outlet temperature of the return pipeline q, respectively; $\mathrm{T}_{q,\tau}^{\mathrm{a}}$ is the ambient temperature of pipe q.

3.3 Coupling Component Constraints

The coupling elements are mainly CHP units and EHP units. In the system scheduling, the CHP unit mostly adopts the back-pressure CHP, and here the extraction CHP with stronger regulation capacity is used, and its operation constraints can be represented by a quadrilateral, as shown in Figure 4.

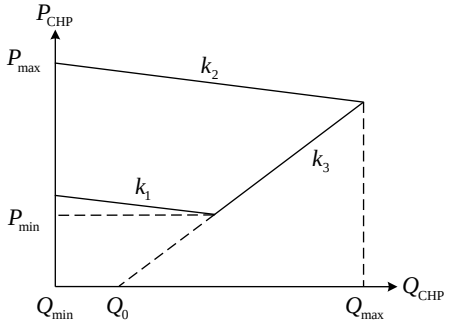

Figure 4. Electrothermal characteristics of CHP units

The constraints on the heating power and electrical power output of the CHP unit are shown in equation (24) and equation (25), respectively.

$$0 \le Q_{i,\tau}^{\mathrm{CHP,adj}} \le Q_{i,\tau}^{\mathrm{CHP,max}} \tag{24}$$

$$\max\left\{P_{i,t}^{\mathrm{CHP,min}} - k_{1,i}Q_{i,\tau}^{\mathrm{CHP,adj}}, k_{3,i}(Q_{i,\tau}^{\mathrm{CHP,adj}} - Q_0)\right\} \le P_{i,t}^{\mathrm{CHP,adj}} \le P_{i,t}^{\mathrm{CHP,max}} - k_{2,i}Q_{i,\tau}^{\mathrm{CHP,adj}} \tag{25}$$

Where: $Q_{i,\tau}^{\mathrm{CHP,max}}$ is the maximum heating power of CHP unit i; $Q_{i,t}^{\mathrm{CHP,adj}}$ and $P_{i,t}^{\mathrm{CHP,adj}}$ is the heating power and generating power of CHP unit i in the feasible domain; $k_{1,i}$, $k_{2,i}$, $k_{3,i}$ are the slopes of the boundaries of the electric and thermal characteristics of CHP unit i; $P_{i,t}^{\mathrm{CHP,max}}$ and $P_{i,t}^{\mathrm{CHP,min}}$ are the maximum and minimum values of the generating power of CHP unit i are respectively.

the EHP unit is a device that consumes electricity to generate heat, and its constraint is:

$$Q_{i,\tau}^{\mathrm{EHP}} = \alpha_i^{\mathrm{EHP}} P_{i,t}^{\mathrm{EHP}} \tag{26}$$

Where: α_i^{EHP} is the power-to-heat efficiency of EHP unit i.

4. Method and Indicators of IEHS Reliability Assessmen

In this paper, a reliability evaluation method for considering the uncertainty of wind, solar and load for multi-state units is proposed, and the definitions and calculation formulas of IEHS reliability indicators Loss of Load Probability (LOLP) and Expected Energy Not Suppled (EENS) are given.

ISSN: 2414-1895 DOI: 10.6919/ICJE.202405_10(5).0037

4.1 IEHS Reliability Assessment Method

Based on the optimal load reduction model and the multi-state model of CHP units, considering the uncertainty of the output and load of wind power and photovoltaic units, the reliability assessment of IEHS is carried out by Monte Carlo simulation method, and the specific steps are as follows, as shown in Figure 5.

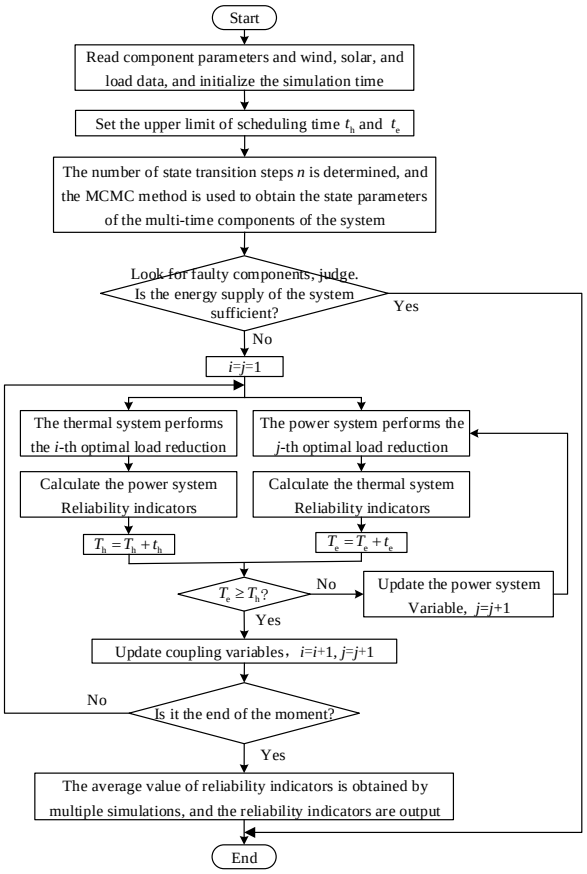

Figure 5. Reliability assessment process of IEHS

4.2 LOLP

The meaning of this metric is the probability that the system will experience load shedding on average per year, and its formula is as follows:

$$LOLP_{e,s} = \frac{1}{N}\sum_{i=1}^{N}\left(\sum_{x\in\Omega_x} p(x)\cdot If\left(\Delta P_{e,s}(x)>0\right)\right) \tag{27}$$

$$LOLP_{h,s} = \frac{1}{N}\sum_{i=1}^{N}\left(\sum_{x\in\Omega_x} p(x)\cdot If\left(\Delta Q_{h,s}(x)>0\right)\right) \tag{28}$$

$$LOLP_{s} = \frac{1}{N}\sum_{i=1}^{N}\left(\sum_{x\in\Omega_x} p(x)\cdot\left(If\left(\Delta P_{e,s}(x)>0\right)\,||\,If\left(\Delta Q_{h,s}(x)>0\right)\right)\right) \tag{29}$$

ISSN: 2414-1895 DOI: 10.6919/ICJE.202405_10(5).0037

Where: N is the total number of sampling years; Ω_x is a collection of all scenes; $p(x)$ is the probability of scenario x; $LOLP_{e,s}$, $LOLP_{h,s}$ and $LOLP_s$ are the probability of power grid power loss load, heat network heat loss load probability and system load loss probability respectively.

4.3 EENS

The meaning of this indicator is the expected value of the system's average annual energy supply shortfall, and its calculation formula is:

$$EENS_{e,s} = \frac{8760}{N}\sum_{i=1}^{N}\left(\sum_{x\in\Omega_x} p(x)\cdot\Delta P_{e,s}(x)\right) \tag{30}$$

$$EENS_{h,s} = \frac{8760}{N}\sum_{i=1}^{N}\left(\sum_{x\in\Omega_x} p(x)\cdot\Delta Q_{h,s}(x)\right) \tag{31}$$

$$EENS_s = \omega_e EENS_{e,s} + \omega_h EENS_{h,s} \tag{32}$$

Where: $EENS_{e,s}$, $EENS_{h,s}$ and $EENS_s$ are expected to be insufficient for the total energy supply of electricity, heat and the system, respectively.

5. Case Simulation

5.1 Summary of the Example

The IEHS constructed in this paper is composed of a 24-node power system and a 32-node thermal system, and its topology is shown in Figure 6. Among them, the power grid data comes from the Matpower toolbox, and the heat network data comes from the reference [9].

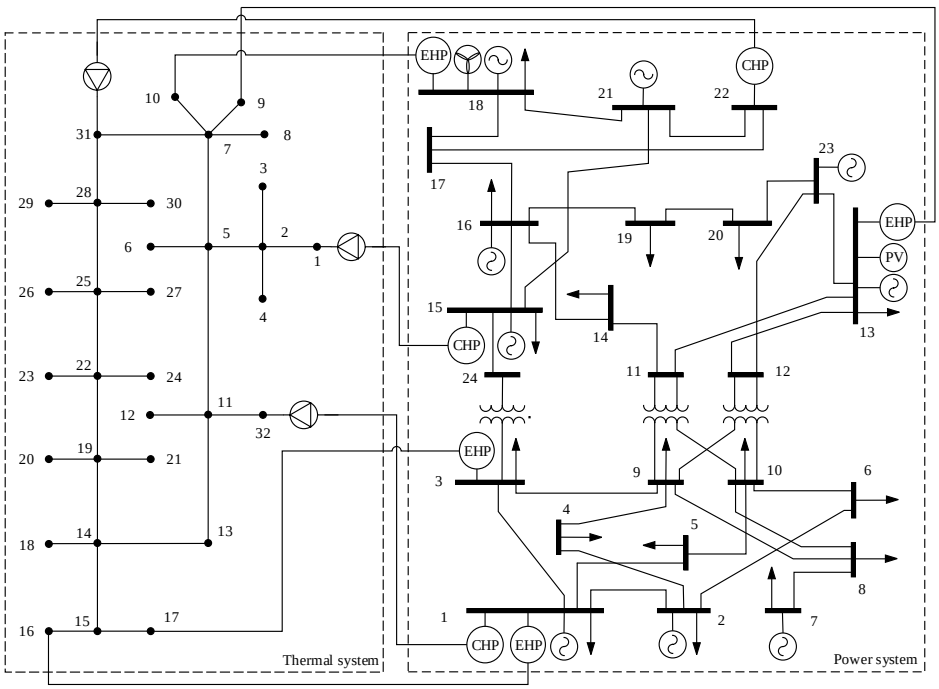

Figure 6. Topology of IEHS

ISSN: 2414-1895 DOI: 10.6919/ICJE.202405_10(5).0037

5.2 Analysis of Optimal Load Reduction Scheduling at Multi-Time Scale

In order to observe the specific situation of multi-time scale scheduling in IEHS reliability evaluation, the scheduling time of heat network system is set to 60 minutes, and the scheduling time of power system is 15 minutes, and the total number of control quantity adjustments under the unified time scale is compared, as shown in Table 1. One of the optimizations is the adjustment of the output of each component in the scheduling process, as shown in Figure 7.

Table 1. Comparison of control quantity adjustment time under different scheduling methods

Time scale	The number of times the power system is dispatched	The number of times the thermal utility system is scheduled	The total number of control volume adjustments
Unify time scales	236	236	3584
Multi-time scales	236	59	2108

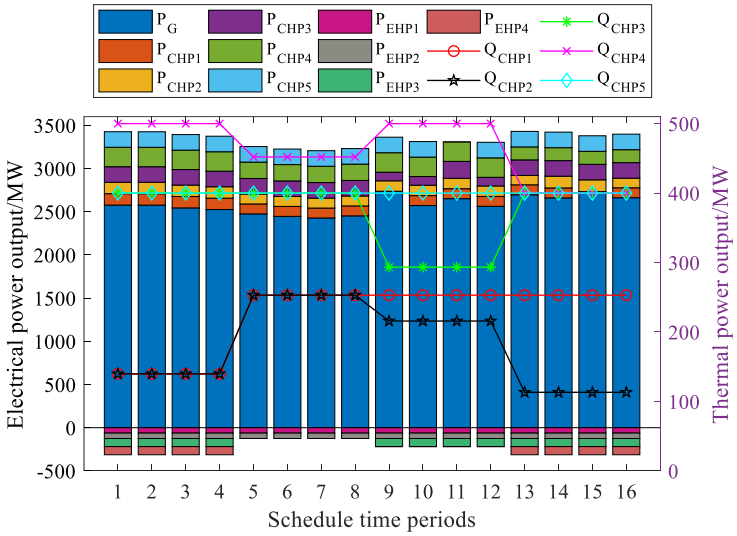

Figure 7. Variation of the output of each control quantity over time

It can be seen from Table 2 and Figure 7 that compared with the optimal scheduling of unified time scale, the optimal scheduling of multiple time scales can reduce the number of system control adjustments and reduce the unit adjustment cost while ensuring the optimization effect, which offers superior economy and aligns more closely with the actual operation of the system. The output of the heat source unit changes greatly in each cycle, which is due to the fact that the output of the new energy unit makes the electric output of the CHP unit change every moment, and the thermal output is constrained by constraints (24) and constraints (25) and adjusted accordingly. Within the time frame of thermal system scheduling, the power system can undergo multiple optimization iterations, thereby minimizing the frequency of heat source output adjustments and eliminating redundant calculations.

5.3 The Impact of the State Transfer Steps on the Reliability of the System

By adjusting the number of state transition steps, the change of the multi-step transition model on the system reliability index is analyzed, and the simulation results are shown in Figure 8.

ISSN: 2414-1895 DOI: 10.6919/ICJE.202405_10(5).0037

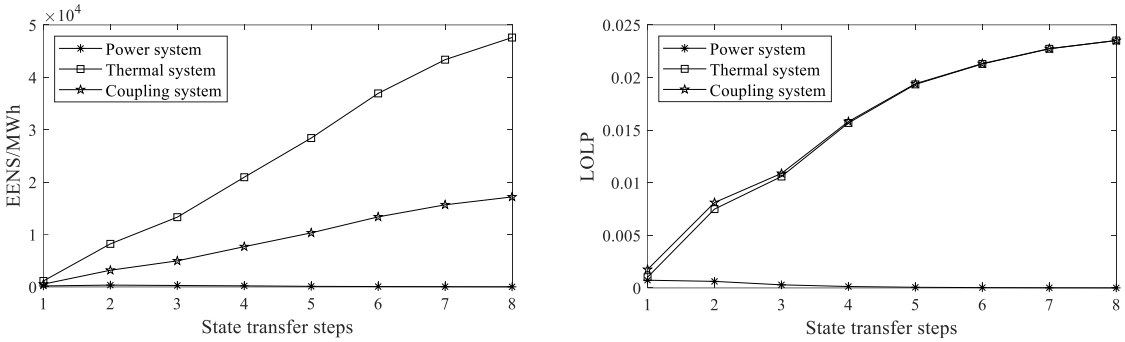

(a) Changes in EENS for different systems (b) Changes in LOLP for different systems

Figure 8. Changes in reliability metrics under different transition steps

It can be seen from Figure 8 that with the increase of the number of transfer steps, the reliability evaluation index of the thermal power system continues to increase, the reliability index of the coupling system and the change of the reliability index of the thermal system are consistent, and the reliability index of the power system does not change much, because the probability of component outage increases with the increase of the number of state transfer steps, and the thermal system is constrained by the output of the heat source is larger, and the power system can maintain normal operation in the case of faulty components by adjusting the output of the generator due to the relatively large additional capacity of the generator. Therefore, when considering the number of multi-state transfer steps, it is necessary to determine the appropriate number of state transfer steps to prevent the system from being susceptible to external interference due to too much degradation of system reliability.

6. Conclusion

Based on the Markov process, a multi-time state probability model for multi-step state transition, a seven-state uncertainty model for load, and an IEHS optimal load reduction model considering multiple time scales are established, and an IEHS reliability evaluation method considering multiple time scales and multi-step state transitions is proposed. The following conclusions are drawn from the simulation results:1) Compared with the unified time scale, considering the multi-time scale dispatching power system, the optimal load reduction can be completed many times, while the heat system will wait for the power system to dispatch multiple times due to the long scheduling time, and determine the heat source output more accurately. 2) With the increase of the number of state transition steps, the probability of component outage is increasing, but the reliability of the coupling system is decreasing, and the reliability of the thermal system is seriously affected.

References

[1] Shu Y.B., Zhang Z.G., Guo J.B., et al. Study on key factors and solution of renewable energy accommodation[J]. Proceedings of the CSEE, 2017, 37(01): 1-9.

[2] Mukherjee U., Walker S., Maroufmashat A., et al. Development of a pricing mechanism for valuing ancillary, transportation and environmental services offered by a power to gas energy system[J]. Energy, 2017, 128: 447-462.

[3] Jia H.P., Ding Y., Song Y.H., et al. Review of reliability analysis for integrated energy systems with integration of cyber physical systems[J]. Power System Technology, 2019, 43(01): 1-11.

[4] Ni W., Lü L., Xiang Y., et al. Reliability evaluation of integrated energy system based on Markov process Monte Carlo method[J]. Power System Technology, 2020, 44(01): 150-158.

[5] Ding Y., Shao C.Z., Hu B., et al. Operational reliability assessment of integrated heat and electricity systems considering the load uncertainties[J]. IEEE Transactions on Smart Grid, 2021, 12(05): 3928-3939.

ISSN: 2414-1895 DOI: 10.6919/ICJE.202405_10(5).0037

[6] Huan J.J., Zhang X.H., Huang X.J., et al. Asset utilization efficiency analysis of integrated energy system considering load uncertainty and operation reliability[J]. Southern Power System Technology, 2021, 15(02): 56-63.

[7] Zhang W.X., Han X.Q., Song S.Y., et al. Operational reliability evaluation of wind integrated power systems based on Markov chain considering uncertainty factors of source-grid-load[J]. Power System Technology, 2018, 42(03): 762-771.

[8] Wang S.P., Zhang S.X., Cheng H.Z., et al. Reliability indices and evaluation method of integrated energy system considering thermal comfort level of customers[J]. Automation of Electric Power Systems, 2023, 47(01): 86-95.

[9] Wang W.X., Hu W., Sun G.Q., et al. Interval energy flow calculation method of integrated electro-thermal system[J]. Power System Technology, 2019, 43(01): 83-95.